WIRELESS COMMUNICATIONS AND MOBILE COMPUTING
Wirel. Commun. Mob. Comput. (2012)
Published online in Wiley Online Library (wileyonlinelibrary.com). DOI: 10.1002/wcm.2334

SPECIAL ISSUE PAPER

Recursive QR packet combining for uplink single-carrier multi-user MIMO HARQ using near ML detection

Tetsuya Yamamoto[1*], Koichi Adachi[2], Sumei Sun[2] and Fumiyuki Adachi[1]

[1] Department of Communications Engineering, Graduate School of Engineering, Tohoku University, 6-6-05 Aza-Aoba, Aramaki, Aoba-ku, Sendai, 980-8579 Japan
[2] Institute for Infocomm Research, A*STAR, 1 Fusionopolis Way, #21-01, Connexis (South Tower), Singapore 138632

ABSTRACT

QR decomposition-based near maximum likelihood block detection significantly improves the transmission performance of uplink single-carrier (SC) multi-user multiple-input multiple-output (MU-MIMO). Hybrid automatic repeat request (HARQ) is an indispensable error control technique for high-quality packet data transmission. The achievable diversity gain of HARQ depends on the packet combining strategy. In uplink MU-MIMO HARQ, the received signal may consist of new packets and retransmitted packets as retransmission for each user acts independently. In this paper, a recursive QR packet combining scheme suitable for uplink SC MU-MIMO HARQ is proposed, which takes into account the number of retransmissions for each user in the detection order. The computational complexity and required storage size can be significantly reduced by the proposed scheme. Moreover, it improves the packet error rate performance and throughput performance significantly over the conventional bit-level log likelihood ratio packet combining, as shown by our computer simulation results. Copyright © 2012 John Wiley & Sons, Ltd.

KEYWORDS
single-carrier; MU-MIMO; HARQ; packet combining; QR decomposition; M-algorithm

***Correspondence**
Tetsuya Yamamoto, Department of Communications Engineering, Graduate School of Engineering, Tohoku University, 6-6-05 Aza-Aoba, Aramaki, Aoba-ku, Sendai, 980-8579 Japan.
E-mail: yamamoto@mobile.ecei.tohoku.ac.jp

1. INTRODUCTION

In next generation mobile data communication systems, high-data-rate transmission is demanded. Multiple-input multiple-output (MIMO) spatial multiplexing [1] provides high-data-rate without increasing the signal bandwidth. For uplink (mobile terminal to base station) data communication, single-carrier (SC) transmission is suitable because of its lower peak-to-average power ratio property [2,3] than multi-carrier transmission, for example, orthogonal frequency division multiplexing [4]. Thus, SC MIMO has been adopted as the uplink transmission technique for Third Generation Partnership Project Long-Term Evolution Advanced system [5].

Since the wireless channel becomes severely frequency-selective as the transmission data rate increases [6], SC MIMO suffers from inter-symbol interference (ISI) arising from the severe frequency-selectivity of the channel. To tackle ISI, QR decomposition and M-algorithm-based near maximum likelihood (ML) block detection (QRM-MLBD) was proposed [7,8]. QRM-MLBD significantly improves the transmission performance of SC MIMO systems in a frequency-selective fading channel with significantly lower computational complexity than ML detection. To enhance the system capacity, multi-user (MU)-MIMO is an effective technique [9,10]. In MU-MIMO, multiple users' signals are spatially multiplexed and decomposed at the receiver. By applying QRM-MLBD to MU-MIMO, the transmission performance of uplink SC MU-MIMO can be significantly improved [11].

Packet access will be the core technology of the next generation mobile data communication systems. High-speed packet transmissions can be realized by the joint use of MIMO systems and hybrid automatic repeat request (HARQ). There are several HARQ protocols, mainly type I HARQ and type II HARQ. In type I HARQ, when decoding error occurs, the same packet is retransmitted until it is correctly received. Packet combining is then

implemented. In type II HARQ, different redundancy bits are used in retransmission. Therefore, type I HARQ is simpler to implement and requires less storage than type II HARQ, and it achieves only diversity gain, whereas type II HARQ achieves both diversity and coding gains at the cost of storage and implementation complexity [12]. Therefore, the packet combining scheme is especially critical to the performance of type I HARQ. The recursive QR packet combining (R-QRPC) [13] obtains the optimal packet combining gain as it optimally incorporates packet combining into QR decomposition. In [14], we proposed a near ML block detection with R-QRPC and M-algorithm for single-user (SU)-MIMO. It was shown that the R-QRPC can significantly increase the throughput performance of SU-MIMO HARQ compared with the bit-level log likelihood ratio (LLR) packet combining [15].

As MU-MIMO technique is essential for system capacity improvement, we are motivated to apply R-QRPC to SC MU-MIMO. In the SC SU-MIMO in [15], a single-channel encoder is assumed, and hence, the received signal always consists of either new packet or retransmitted packet. On the other hand, in uplink MU-MIMO HARQ, the received signal may consist of new packets and retransmitted packets as retransmission for each user acts independently. Therefore, the R-QRPC needs to be re-designed for the MU case. In this paper, we present an R-QRPC for SC MU-MIMO HARQ, which can reduce the computational complexity and storage requirement significantly over the conventional scheme. As HARQ is independently carried out among users, the received signal may consist of packets with different number of retransmissions. In such a case, the packet combining gain differs among the transmitted signals. Hence, the detection order of transmitted signals may affect the individual packet error rate (PER) performance. In this paper, we will consider the effect of detection ordering between retransmitted and newly transmitted packets. We evaluate by computer simulation the PER and throughput performances of SC MU-MIMO HARQ with the QRM-MLBD using the R-QRPC and show that significant performance improvement can be achieved by our proposed scheme, on top of the complexity and storage saving.

The rest of the paper is organized as follows. In Section 2, system model of SC MU-MIMO HARQ is presented. Section 3 describes the R-QRPC for MU-MIMO HARQ. In Section 4, the simulation results are presented, and finally, Section 5 concludes the paper.

2. SYSTEM MODEL

2.1. General transmission procedure

In this paper, a synchronous slotted U-user MU-MIMO packet transmission is considered, where one packet is composed of multiple data blocks and the slot length is the same as the packet length. Figure 1 illustrates the transmitter/receiver structure considered in this paper, where the block size and guard interval length are denoted

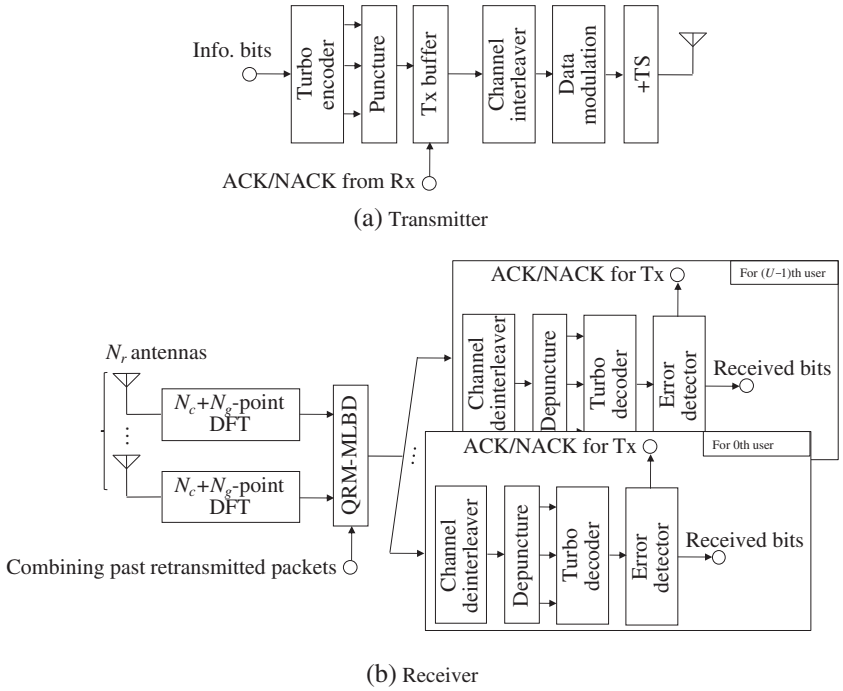

Figure 1. System model. DFT, discrete Fourier transform; QRM-MLBD, QR decomposition and M-algorithm-based near maximum likelihood block detection.

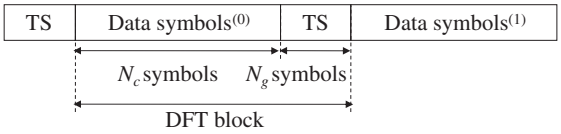

Figure 2. Transmit block structure. TS, training sequence; DFT, discrete Fourier transform.

by N_c and N_g, respectively. Each user is equipped with a single transmit antenna, and the base station is equipped with N_r receive antennas. We assume that, at every slot, each user always has one packet to transmit.

All U users employ the type I HARQ. At each user terminal, after channel coding and puncturing, the coded bit sequence is stored in the transmitter buffer. The coded bit sequence is transformed into a data-modulated symbol sequence, which is divided into a sequence of symbol blocks of N_c symbols each. The transmit block structure is illustrated in Figure 2. Prior to the transmission, the training sequence (TS) of length N_g [16,17] is appended at the last part of each block instead of the well-known cyclic prefix as TS can reduce the detection complexity of QRM-MLBD [8]. After the insertion of TS, the signal block is transmitted.

The transmitted block of each user propagates through different channels and is superimposed at the N_r receive antennas at the base station. The received signal block is transformed into the frequency-domain signal by an $(N_c + N_g)$-point discrete Fourier transform (DFT). QRM-MLBD and packet combining are jointly carried out to output LLR sequence. Finally, channel decoding is performed by using the LLR output to recover each user's data sequence. For a particular user, if its packet is correctly received, then a positive acknowledgment (ACK) signal is sent back to the user. If any error is detected in the decoded sequence, a negative acknowledgment (NACK) is sent back to request for retransmission of the same packet.

2.2. Transmit signal and received signal representations

The packet index of the uth user is denoted by n_u. The coded bit sequence is divided into N_b blocks with a sequence of N_c symbols each. The n_bth data symbol block within the n_uth packet can be expressed using the vector form as $\mathbf{d}_u^{(n_u,n_b)} = \left[d_u^{(n_u,n_b)}(0), \ldots, d_u^{(n_u,n_b)}(t), \ldots, d_u^{(n_u,n_b)}(N_c-1)\right]^T$, where $(\cdot)^T$ expresses the transposition. After TS addition, the block $\mathbf{s}_u^{(n_u,n_b)} = \left[s_u^{(n_u,n_b)}(0), \ldots, s_u^{(n_u,n_b)}(t), \ldots, d_u^{(n_u,n_b)}(N_c+N_g-1)\right]^T$ to be transmitted is expressed as

$$\begin{aligned}\mathbf{s}_u^{(n_u,n_b)} &= \left[d_u^{(n_u,n_b)}(0), \ldots, d_u^{(n_u,n_b)}(N_c-1), x_u(0), \right. \\ &\qquad \left. \ldots, x_u(N_g-1)\right]^T \\ &= \begin{bmatrix} \mathbf{d}_u^{(n_u,n_b)} \\ \mathbf{x}_u \end{bmatrix} \end{aligned} \tag{1}$$

where $\mathbf{x}_u = [x_u(0), \ldots, x_u(t), \ldots, x_u(N_g-1)]^T$ denotes the TS vector which is identical for all blocks.

Let us consider the pth slot. The frequency-domain-received signal vector at the n_rth receive antenna during the n_bth block $\mathbf{Y}_{n_r}^{(p,n_b)} = \left[Y_{n_r}^{(p,n_b)}(0), \ldots, Y_{n_r}^{(p,n_b)}(k), \ldots, Y_{n_r}^{(p,n_b)}(N_c+N_g-1)\right]^T$, $n_r = 0 \sim (N_r-1)$, is expressed as [8]

$$\mathbf{Y}_{n_r}^{(p,n_b)} = \sum_{u=0}^{U-1} \sqrt{2S_u}\mathbf{H}_{u,n_r}^{(p)}\mathbf{F}\mathbf{s}_u^{(n_u,n_b)} + \mathbf{N}_{n_r}^{(p)} \tag{2}$$

where S_u is the average received signal power of the uth user, $\mathbf{F}$ is the DFT matrix of size $(N_c+N_g)\times(N_c+N_g)$ [8], $\mathbf{s}_u^{(n_u,n_b)}$ is the n_bth data block within the n_uth packet, and $\mathbf{N}_{n_r}^{(p)} \sim CN(\mathbf{0}, 2\sigma^2\mathbf{I}_{N_c+N_g})$ is the $(N_c+N_g)\times 1$ zero-mean additive white Gaussian noise vector. $\mathbf{I}_A$ represents the $A \times A$ identity matrix. $\mathbf{H}_{u,n_r}^{(p)}$ is the frequency-domain channel matrix between the uth user and the n_rth receive antenna in the pth slot [8].

The received signal at each receive antenna is stacked to form an $N_r(N_c+N_g)\times 1$ stacked frequency-domain received signal $\mathbf{Y}^{(p,n_b)} = \left[\left\{\mathbf{Y}_0^{(p,n_b)}\right\}^T, \ldots, \left\{\mathbf{Y}_{N_r-1}^{(p,n_b)}\right\}^T\right]^T$ as

$$\begin{aligned}\mathbf{Y}^{(p,n_b)} = \mathbf{G}^{(p)} &\left[\left\{\mathbf{s}_0^{(n_0,n_b)}\right\}^T, \ldots, \left\{\mathbf{s}_u^{(n_u,n_b)}\right\}^T, \ldots, \right. \\ &\left. \left\{\mathbf{s}_{U-1}^{(n_{U-1},n_b)}\right\}^T\right]^T + \mathbf{N}^{(p)} \end{aligned} \tag{3}$$

where $\mathbf{N}^{(p)}$ is the $N_r(N_c+N_g)\times 1$ stacked noise vector and $\mathbf{G}^{(p)}$ is an equivalent channel matrix of size $N_r(N_c+N_g)\times U(N_c+N_g)$, which is a concatenation of the space and frequency-domain channel and DFT given by

$$\mathbf{G}^{(p)} = \begin{bmatrix} \sqrt{2S_0}\mathbf{H}_{0,0} & \cdots & \sqrt{2S_{U-1}}\mathbf{H}_{U-1,0} \\ \vdots & \ddots & \vdots \\ \sqrt{2S_0}\mathbf{H}_{0,N_r-1} & \cdots & \sqrt{2S_{U-1}}\mathbf{H}_{U-1,N_r-1} \end{bmatrix} \begin{bmatrix} \mathbf{F} & & \\ & \ddots & \\ & & \mathbf{F} \end{bmatrix} \tag{4}$$

$\mathbf{N}^{(p)}$ is the $N_r(N_c+N_g)\times 1$ overall noise vector.

3. RECURSIVE QR PACKET COMBINING FOR MU-MIMO HARQ

In this section, the R-QRPC for SC MU-MIMO HARQ is presented. The following two cases need to be considered:

Case 1. *All users are in retransmission mode, and the number of retransmissions is the same for all users.*

Case 2. *Some users in retransmission mode and the others transmit a new packet.*

3.1. Case 1

Since the number of retransmissions is the same for all users, the derivation of R-QRPC is similar to the SU-MIMO system [14].

Suppose each user transmits the n_uth packet in the pth slot, $p = 0 \sim P$. The stacked frequency-domain received signal vector in the pth slot $\mathbf{Y}^{(p)}$ is expressed as

$$\mathbf{Y}^{(p,n_b)} = \mathbf{G}^{(p)} \left[\left\{ \mathbf{s}_0^{(n_0,n_b)} \right\}^T, \ldots, \left\{ \mathbf{s}_u^{(n_u,n_b)} \right\}^T, \ldots, \left\{ \mathbf{s}_{U-1}^{(n_{U-1},n_b)} \right\}^T \right]^T + \mathbf{N}^{(p,n_b)} \tag{5}$$

3.1.1. Expanded QR packet combining.

First, let us define the expanded received signal vector $\overline{\mathbf{Y}}^{(P,n_b)}$ of size $(P+1)N_r(N_c+N_g) \times 1$ as

$$\begin{aligned} \overline{\mathbf{Y}}^{(P,n_b)} &= \begin{bmatrix} \mathbf{Y}^{(0,n_b)} \\ \vdots \\ \mathbf{Y}^{(P,n_b)} \end{bmatrix} \\ &= \begin{bmatrix} \mathbf{G}^{(0)} \\ \vdots \\ \mathbf{G}^{(P)} \end{bmatrix} \begin{bmatrix} \mathbf{s}_0^{(n_0,n_b)} \\ \vdots \\ \mathbf{s}_{U-1}^{(n_{U-1},n_b)} \end{bmatrix} + \begin{bmatrix} \mathbf{N}^{(0,n_b)} \\ \vdots \\ \mathbf{N}^{(P,n_b)} \end{bmatrix} \\ &= \overline{\mathbf{G}}^{(P)} \left[\left\{ \mathbf{s}_0^{(n_0,n_b)} \right\}^T, \ldots, \left\{ \mathbf{s}_{U-1}^{(n_{U-1},n_b)} \right\}^T \right]^T + \overline{\mathbf{N}}^{(P,n_b)} \end{aligned} \tag{6}$$

where $\overline{\mathbf{G}}^{(P)}$ is the expanded channel matrix of size $(P+1)N_r(N_c+N_g) \times U(N_c+N_g)$.

To achieve the optimal packet combining gain, expanded QR packet combining (E-QRPC) [14], which is a straightforward application of the QR decomposition to all the received retransmitted packets can be used. In E-QRPC, QR decomposition is applied to the expanded channel matrix $\overline{\mathbf{G}}^{(P)}$ to obtain $\overline{\mathbf{G}}^{(P)} = \overline{\mathbf{Q}}^{(P)}\overline{\mathbf{R}}^{(P)}$, where $\overline{\mathbf{Q}}^{(P)}$ is a $(P+1)N_r(N_c+N_g) \times U(N_c+N_g)$ unitary matrix and $\overline{\mathbf{R}}^{(P)}$ is an $U(N_c+N_g) \times U(N_c+N_g)$ upper triangular matrix. The transformed received signal $\hat{\mathbf{Y}}^{(P,n_b)}$ is obtained as

$$\begin{aligned} \hat{\mathbf{Y}}^{(P,n_b)} &= \left\{ \overline{\mathbf{Q}}^{(P)} \right\}^H \overline{\mathbf{Y}}^{(P,n_b)} \\ &= \overline{\mathbf{R}}^{(P)} \left[\left\{ \mathbf{s}_0^{(n_0,n_b)} \right\}^T, \ldots, \left\{ \mathbf{s}_{U-1}^{(n_{U-1},n_b)} \right\}^T \right]^T \\ &\quad + \left\{ \overline{\mathbf{Q}}^{(P)} \right\}^H \overline{\mathbf{N}}^{(P,n_b)} \end{aligned} \tag{7}$$

From Equation (7), the ML solution is equivalent to selecting the path with the minimum Euclidean distance in a tree diagram with $U(N_c+N_g)$ stages. This can be realized by M-algorithm. At each stage, the best M surviving paths selected from all the paths are passed to the next stage. The squared Euclidean distance is used for branch metric calculation. The obtained bit LLRs are input to the channel decoder. However, the LLR values may not be able to be directly computed because surviving paths at the last stage do not necessarily contain both 1 and 0 for every coded bit. To compensate for this loss, in this paper, we adopt the LLR computation method proposed in [18].

Although this E-QRPC can achieve the optimal packet combining gain, all the retransmitted packets and the associated channel matrices need to be stored. This brings huge memory size of the receiver. Furthermore, the size of the expanded channel matrix to which the QR decomposition is applied becomes $(P+1)N_r(N_c+N_g) \times U(N_c+N_g)$, and therefore, the computational complexities required for the QR decomposition and generation of the transformed signal grow with the number of retransmissions.

3.1.2. Recursive QR packet combining.

To reduce the required computational complexity and memory size, an R-QRPC is proposed in [13]. The expanded channel matrix in the Pth slot $\overline{\mathbf{G}}^{(P)}$ can be expressed by using $\overline{\mathbf{G}}^{(P-1)}$ and $\mathbf{G}^{(P)}$ as

$$\overline{\mathbf{G}}^{(P)} = \begin{bmatrix} \overline{\mathbf{G}}^{(P-1)} \\ \mathbf{G}^{(P)} \end{bmatrix} \tag{8}$$

Then, $\overline{\mathbf{G}}^{(P)}$ can be rewritten, using the relationship $\overline{\mathbf{G}}^{(P-1)} = \overline{\mathbf{Q}}^{(P-1)}\overline{\mathbf{R}}^{(P-1)}$, as

$$\begin{aligned} \overline{\mathbf{G}}^{(P)} &= \begin{bmatrix} \overline{\mathbf{Q}}^{(P-1)}\overline{\mathbf{R}}^{(P-1)} \\ \mathbf{G}^{(P)} \end{bmatrix} \\ &= \begin{bmatrix} \overline{\mathbf{Q}}^{(P-1)} & \mathbf{0} \\ \mathbf{0} & \mathbf{I}_{N_r(N_c+N_g)} \end{bmatrix} \begin{bmatrix} \overline{\mathbf{R}}^{(P-1)} \\ \mathbf{G}^{(P)} \end{bmatrix} \end{aligned} \tag{9}$$

Applying QR decomposition to $\begin{bmatrix} \overline{\mathbf{R}}^{(P-1)} \\ \mathbf{G}^{(P)} \end{bmatrix}$ in Equation (9), we have

$$\begin{bmatrix} \overline{\mathbf{R}}^{(P-1)} \\ \mathbf{G}^{(P)} \end{bmatrix} = \mathbf{Q}^{(P)}\mathbf{R}^{(P)} \tag{10}$$

Now, $\mathbf{Q}^{(P)}$ is an $(N_r(N_c+N_g)+U(N_c+N_g))\times U(N_c+N_g)$ unitary matrix and $\mathbf{R}^{(P)}$ is a $U(N_c+N_g)\times U(N_c+N_g)$ upper triangular matrix. Finally, from Equations (8)–(10), we have

$$\overline{\mathbf{G}}^{(P)}=\begin{bmatrix}\overline{\mathbf{Q}}^{(P-1)} & \mathbf{0}\\ \mathbf{0} & \mathbf{I}_{N_r(N_c+N_g)}\end{bmatrix}\mathbf{Q}^{(P)}\mathbf{R}^{(P)} \quad (11)$$

Since $\mathbf{Q}^{(P)}$ and $\begin{bmatrix}\overline{\mathbf{Q}}^{(P-1)} & \mathbf{0}\\ \mathbf{0} & \mathbf{I}_{N_r(N_c+N_g)}\end{bmatrix}$ are both unitary, $\begin{bmatrix}\overline{\mathbf{Q}}^{(P-1)} & \mathbf{0}\\ \mathbf{0} & \mathbf{I}_{N_r(N_c+N_g)}\end{bmatrix}\mathbf{Q}^{(P)}$ is also unitary. Therefore, the expanded received signal vector $\overline{\mathbf{Y}}^{(P,n_b)}$ of Equation (6) can be transformed as

$$\overline{\mathbf{Y}}^{(P,n_b)}=\begin{bmatrix}\mathbf{Y}^{(0,n_b)}\\ \vdots\\ \mathbf{Y}^{(P-1,n_b)}\\ \mathbf{Y}^{(P,n_b)}\end{bmatrix}=\begin{bmatrix}\mathbf{G}_0^{(0)} & \cdots & \mathbf{G}_{U-1}^{(0)} & \mathbf{0}\\ \vdots & \ddots & \vdots & \vdots\\ \mathbf{G}_0^{(P-1)} & \cdots & \mathbf{G}_{U-1}^{(P-1)} & \mathbf{0}\\ \mathbf{G}_0^{(P)} & \cdots & \mathbf{0} & \mathbf{G}_{U-1}^{(P)}\end{bmatrix}\begin{bmatrix}\mathbf{s}_0^{(n_0,n_b)}\\ \vdots\\ \mathbf{s}_{U-1}^{(n_{U-1},n_b)}\\ \mathbf{s}_{U-1}^{(n_{U-1}+1,n_b)}\end{bmatrix}+\begin{bmatrix}\mathbf{N}^{(0,n_b)}\\ \vdots\\ \mathbf{N}^{(P,n_b)}\end{bmatrix} \quad (13)$$

$$\begin{aligned}\hat{\mathbf{Y}}^{(P,n_b)}&=\left\{\begin{bmatrix}\overline{\mathbf{Q}}^{(P-1)} & \mathbf{0}\\ \mathbf{0} & \mathbf{I}_{N_r(N_c+N_g)}\end{bmatrix}\mathbf{Q}^{(P)}\right\}^H\begin{bmatrix}\overline{\mathbf{Y}}^{(P-1,n_b)}\\ \mathbf{Y}^{(P,n_b)}\end{bmatrix}\\ &=\left\{\mathbf{Q}^{(P)}\right\}^H\begin{bmatrix}\left\{\overline{\mathbf{Q}}^{(P-1)}\right\}^H\overline{\mathbf{Y}}^{(P-1,n_b)}\\ \mathbf{Y}^{(P,n_b)}\end{bmatrix}=\left\{\mathbf{Q}^{(P)}\right\}^H\begin{bmatrix}\hat{\mathbf{Y}}^{(P-1,n_b)}\\ \mathbf{Y}^{(P,n_b)}\end{bmatrix}\end{aligned} \quad (12)$$

Equation (12) implies that the transformed signal vector $\hat{\mathbf{Y}}^{(P,n_b)}$ in Equation (7) can be obtained recursively using the previously obtained transformed vector $\hat{\mathbf{Y}}^{(P-1,n_b)}$ and the present stacked frequency-domain received signal vector $\mathbf{Y}^{(P,n_b)}$. Only the previously obtained upper triangular matrix and the present channel matrix are required for the QR decomposition.

$$\tilde{\mathbf{Y}}^{(P,n_b)}=\overline{\mathbf{Y}}^{(P,n_b)}-\begin{bmatrix}\mathbf{G}_1^{(0)}\\ \vdots\\ \mathbf{G}_{U-1}^{(P-1)}\\ \mathbf{0}\end{bmatrix}\mathbf{s}_{U-1}^{(n_{U-1},n_b)}=\begin{bmatrix}\mathbf{G}_0^{(0)} & \cdots & \mathbf{G}_{U-2}^{(0)} & \mathbf{0}\\ \vdots & \ddots & \vdots & \vdots\\ \mathbf{G}_0^{(P-1)} & \cdots & \mathbf{G}_{U-2}^{(P-1)} & \mathbf{0}\\ \mathbf{G}_0^{(P)} & \cdots & \mathbf{G}_{U-2}^{(P)} & \mathbf{G}_{U-1}^{(P)}\end{bmatrix}\begin{bmatrix}\mathbf{s}_0^{(n_0,n_b)}\\ \vdots\\ \mathbf{s}_{U-2}^{(n_{U-2},n_b)}\\ \mathbf{s}_{U-1}^{(n_{U-1}+1,n_b)}\end{bmatrix}+\begin{bmatrix}\mathbf{N}^{(0,n_b)}\\ \vdots\\ \mathbf{N}^{(P,n_b)}\end{bmatrix} \quad (14)$$

In contrast to the E-QRPC, the R-QRPC does not require to store all the received retransmitted packets and equivalent channel matrices. This contributes to the significant amount of memory saving. The computational complexity required for QR decomposition can also be reduced compared with the E-QRPC when the number of retransmissions is more than two. The size of a matrix to which the QR decomposition is applied is always $(N_r(N_c+N_g)+U(N_c+N_g))\times U(N_c+N_g)$ irrespective of the number of retransmissions when $P\geq 1$. It should be noted that this R-QRPC obtains the same packet combining gain as the E-QRPC with the less memory size and complexity. After the recursive packet combining, M-algorithm is applied to obtain bit LLRs.

3.2. Case 2

Without loss of generality, let us suppose that the $(U-1)$th user retransmits the new packet, that is, the $(n_{U-1}+1)$th packet, whereas the others transmit the same packet.

Based on the stacked frequency-domain received signal vector in Equation (5), the expanded received signal vector $\overline{\mathbf{Y}}^{(P,n_b)}$ can be given by

where $\mathbf{G}^{(p)}$ is partitioned into the $N_r(N_c+N_g)\times(N_c+N_g)$ sub-matrices $\mathbf{G}_u^{(p)}$, which corresponds to the uth user's equivalent channel matrix.

Since $\mathbf{s}_{U-1}^{(n_{U-1},n_b)}$ was successfully received in the $(P-1)$th slot, $\mathbf{s}_{U-1}^{(n_{U-1},n_b)}$ can be canceled as

The QR decomposition in the $(P-1)$th slot is given by

$$\begin{aligned}\overline{\mathbf{G}}^{(P-1)}&=\begin{bmatrix}\overline{\mathbf{G}}_0^{(P-1)} & \cdots & \overline{\mathbf{G}}_{U-1}^{(P-1)}\end{bmatrix}\\ &=\overline{\mathbf{Q}}^{(P-1)}\overline{\mathbf{R}}^{(P-1)}\\ &=\overline{\mathbf{Q}}^{(P-1)}\begin{bmatrix}\overline{\mathbf{R}}_0^{(P-1)} & \cdots & \overline{\mathbf{R}}_{U-1}^{(P-1)}\end{bmatrix}\end{aligned} \quad (15)$$

where $\overline{\mathbf{G}}^{(p)}$ is partitioned into the $pN_r(N_c+N_g)\times(N_c+N_g)$ sub-matrices $\overline{\mathbf{G}}_u^{(p)}$, and $\overline{\mathbf{R}}^{(p)}$ is partitioned into the $U(N_c+N_g)\times(N_c+N_g)$ sub-matrices $\overline{\mathbf{R}}_u^{(p)}$. From Equation (15), the expanded channel matrix in the Pth slot $\overline{\mathbf{G}}^{(P)}$ can be expressed by using $\overline{\mathbf{G}}_u^{(p)}$, $u=0\sim U-2$, and $\mathbf{G}_u^{(P)}$, $u=0\sim U-1$ as

$$\begin{aligned}\overline{\mathbf{G}}^{(P)} &= \begin{bmatrix} \mathbf{G}_0^{(0)} & \cdots & \mathbf{G}_{U-2}^{(0)} & \mathbf{0} \\ \vdots & \ddots & \vdots & \vdots \\ \mathbf{G}_0^{(P-1)} & \cdots & \mathbf{G}_{U-2}^{(P-1)} & \mathbf{0} \\ \mathbf{G}_0^{(P)} & \cdots & \mathbf{G}_{U-2}^{(P)} & \mathbf{G}_{U-1}^{(P)} \end{bmatrix} = \begin{bmatrix} \overline{\mathbf{G}}_0^{(P-1)} & \cdots & \overline{\mathbf{G}}_{U-2}^{(P-1)} & \mathbf{0} \\ \mathbf{G}_0^{(P)} & \cdots & \mathbf{G}_{U-2}^{(P)} & \mathbf{G}_{U-1}^{(P)} \end{bmatrix} \\ &= \begin{bmatrix} \overline{\mathbf{Q}}^{(P-1)}\overline{\mathbf{R}}_0^{(P-1)} & \cdots & \overline{\mathbf{Q}}^{(P-1)}\overline{\mathbf{R}}_{U-2}^{(P-1)} & \mathbf{0} \\ \mathbf{G}_0^{(P)} & \cdots & \mathbf{G}_{U-2}^{(P)} & \mathbf{G}_{U-1}^{(P)} \end{bmatrix} \\ &= \begin{bmatrix} \overline{\mathbf{Q}}^{(P-1)} & \mathbf{0} \\ \mathbf{0} & \mathbf{I}_{N_r(N_c+N_g)} \end{bmatrix} \begin{bmatrix} \overline{\mathbf{R}}_0^{(P-1)} & \cdots & \overline{\mathbf{R}}_{U-2}^{(P-1)} & \mathbf{0} \\ \mathbf{G}_0^{(P)} & \cdots & \mathbf{G}_{U-2}^{(P)} & \mathbf{G}_{U-1}^{(P)} \end{bmatrix}\end{aligned} \tag{16}$$

Applying QR decomposition to $\begin{bmatrix} \overline{\mathbf{R}}_0^{(P-1)} & \cdots & \overline{\mathbf{R}}_{U-2}^{(P-1)} & \mathbf{0} \\ \mathbf{G}_0^{(P)} & \cdots & \mathbf{G}_{U-2}^{(P)} & \mathbf{G}_{U-1}^{(P)} \end{bmatrix}$ in Equation (16) as

$$\begin{bmatrix} \overline{\mathbf{R}}_0^{(P-1)} & \cdots & \overline{\mathbf{R}}_{U-2}^{(P-1)} & \mathbf{0} \\ \mathbf{G}_0^{(P)} & \cdots & \mathbf{G}_{U-2}^{(P)} & \mathbf{G}_{U-1}^{(P)} \end{bmatrix} = \mathbf{Q}^{(P)}\mathbf{R}^{(P)} \tag{17}$$

Finally, from Equations (16) and (17), we have

$$\overline{\mathbf{G}}^{(P)} = \begin{bmatrix} \overline{\mathbf{Q}}^{(P-1)} & \mathbf{0} \\ \mathbf{0} & \mathbf{I}_{N_r(N_c+N_g)} \end{bmatrix} \mathbf{Q}^{(P)}\mathbf{R}^{(P)} \tag{18}$$

The expanded received signal vector after the cancelation of successfully received data from $\tilde{\mathbf{Y}}^{(P,n_b)}$ of Equation (14) can be transformed as

$$\begin{aligned}\hat{\mathbf{Y}}^{(P,n_b)} &= \left\{ \begin{bmatrix} \overline{\mathbf{Q}}^{(P-1)} & \mathbf{0} \\ \mathbf{0} & \mathbf{I}_{N_r(N_c+N_g)} \end{bmatrix} \mathbf{Q}^{(P)} \right\}^H \tilde{\mathbf{Y}}^{(P,n_b)} \\ &= \left\{\mathbf{Q}^{(P)}\right\}^H \begin{bmatrix} \left\{\overline{\mathbf{Q}}^{(P-1)}\right\}^H \left(\overline{\mathbf{Y}}^{(P-1,n_b)} - \overline{\mathbf{G}}_{U-1}^{(P-1)}\mathbf{s}_{U-1}^{(n_{U-1},n_b)}\right) \\ \mathbf{Y}^{(P,n_b)} \end{bmatrix} \\ &= \left\{\mathbf{Q}^{(P)}\right\}^H \begin{bmatrix} \hat{\mathbf{Y}}^{(P-1,n_b)} - \overline{\mathbf{R}}_{U-1}^{(P-1)}\mathbf{s}_{U-1}^{(n_{U-1},n_b)}\right) \\ \mathbf{Y}^{(P,n_b)} \end{bmatrix} = \mathbf{R}^{(P)} \begin{bmatrix} \mathbf{s}_0^{(n_0,n_b)} \\ \vdots \\ \mathbf{s}_{U-2}^{(n_{U-2},n_b)} \\ \mathbf{s}_{U-1}^{(n_{U-1}+1,n_b)} \end{bmatrix}\end{aligned} \tag{19}$$

From Equation (19) in Case 2, the transformed signal vector $\hat{\mathbf{Y}}^{(P,n_b)}$ can also be obtained recursively using $\hat{\mathbf{Y}}^{(P-1,n_b)}$ and $\overline{\mathbf{R}}^{(P-1)}$ from the previous time slot, the received signal vector $\mathbf{Y}^{(P,n_b)}$, and the channel matrix $\mathbf{G}^{(P)}$ from the present slot.

3.3. Detection ordering

In the previous subsection, no ordering was considered; that is, the signal detection is performed in a descending order from the $(U-1)$th user. It is well known that the overall performance of spatial multiplexed system depends on the detection ordering [7,19]. This ordering can also be applied to R-QRPC by arbitrarily swapping the corresponding columns of matrix $\overline{\mathbf{G}}^{(p)}$. In M-algorithm, the accuracy of surviving path selection at early stages significantly affects the overall performance of QRM-MLBD. This is because the M-algorithm successively reduces the number of paths stage-by-stage from the symbols located at the bottom of the transmit symbol vector. Therefore, in this subsection, detection ordering schemes are introduced, which considers the aforementioned case 1 and case 2.

3.3.1. Case 1.

In case 1, since the number of retransmissions is the same for all users, the achievable diversity gain for all users is identical. Thus, the detection ordering schemes for the SU-MIMO system [7,20] can be directly applied. In this paper, we consider the following three detection ordering schemes: *user-first ordering (UFO)*, *code-first ordering (CFO)* [7], and *sorted QR decomposition (SQRD)* [20].

In UFO, the signals are ordered in descending order of received signal-to-noise power ratio (SNR); that is, the signal with highest received SNR is detected first. Since the received SNR is identical for all the symbols within the block in the case of SC block transmission, the ordering is performed for every block as Equation (5). Since fading correlation among symbols transmitted from the same user is one, surviving path selection may be inaccurate especially at early stages [7].

To avoid the above problem, the CFO was proposed [7]. The ordered transmit symbol vector is given by

$$\begin{aligned}\bar{\mathbf{s}}^{\text{order}} &= \left[s_0^{(n_0,n_b)}(0),\ldots,s_{U-1}^{(n_{U-1},n_b)}(0),\ldots,s_0^{(n_0,n_b)}\left(N_c+N_g-1\right),\ldots,s_{U-1}^{(n_{U-1},n_b)}\left(N_c+N_g-1\right)\right]^T \\ &= \left[\left\{\mathbf{d}^{(n_b)}(0)\right\}^T,\ldots,\left\{\mathbf{d}^{(n_b)}(N_c-1)\right\}^T,\mathbf{u}^T(0),\ldots,\mathbf{u}^T(N_g-1)\right]^T\end{aligned} \tag{20}$$

where $\mathbf{d}^{(n_b)}(t) = \left[d_0^{(n_0,n_b)}(t),\ldots,d_{U-1}^{(n_{U-1},n_b)}(t)\right]^T$ and $\mathbf{u}(t) = [u_0(t),u_1(t),\ldots u_{U-1}(t)]^T$ denote the data symbol vector and TS vector at the tth symbol of size $U\times 1$, respectively. In this ordering scheme, the fading correlation among the ordered neighboring symbols becomes lower than that for the UFO. This results in the improved path selection at early stages

SQRD is also known as an effective detection ordering scheme to improve the accuracy of the path selection at early stages [20] by maximizing the diagonal elements in $\mathbf{R}^{(P)}$ from lower right to upper left. However, it requires higher computational complexity for QR decomposition compared to the above two detection ordering schemes.

3.3.2. Case 2.

In case 2, the received signal consists of new packets and retransmitted packets or packets with different number of retransmissions. We can intuitively expect that better performance can be achieved by detecting the combined packet first because of the higher packet combining gain. Therefore, we introduce a detection ordering scheme, which swaps the column of $\overline{\mathbf{G}}^{(p)}$ so that the packet with the larger of retransmissions is detected first.

The expanded received signal vector after the cancelation of successfully received data $\tilde{\mathbf{Y}}^{(P,n_b)}$ in Equation (14) after ordering becomes

$$\tilde{\mathbf{Y}}^{(P,n_b)} = \begin{bmatrix} \mathbf{0} & \mathbf{G}_0^{(0)} & \cdots & \mathbf{G}_{U-2}^{(0)} \\ \vdots & \vdots & \ddots & \vdots \\ \mathbf{0} & \mathbf{G}_0^{(P-1)} & \cdots & \mathbf{G}_{U-2}^{(P-1)} \\ \mathbf{G}_{U-1}^{(P)} & \mathbf{G}_0^{(P)} & \cdots & \mathbf{G}_{U-2}^{(P)} \end{bmatrix} \begin{bmatrix} \mathbf{s}_{U-1}^{(n_{U-1}+1,n_b)} \\ \mathbf{s}_0^{(n_0,n_b)} \\ \vdots \\ \mathbf{s}_{U-2}^{(n_{U-2},n_b)} \end{bmatrix} + \begin{bmatrix} \mathbf{N}^{(0,n_b)} \\ \vdots \\ \mathbf{N}^{(P,n_b)} \end{bmatrix} \tag{21}$$

Similar to Equation (16), the expanded channel matrix in the Pth slot $\overline{\mathbf{G}}^{(P)}$ can be modified as

$$\begin{aligned}\overline{\mathbf{G}}^{(P)} &= \begin{bmatrix} \mathbf{0} & \mathbf{G}_0^{(0)} & \cdots & \mathbf{G}_{U-2}^{(0)} \\ \vdots & \vdots & \ddots & \vdots \\ \mathbf{0} & \mathbf{G}_0^{(P-1)} & \cdots & \mathbf{G}_{U-2}^{(P-1)} \\ \mathbf{G}_{U-1}^{(P)} & \mathbf{G}_0^{(P)} & \cdots & \mathbf{G}_{U-2}^{(P)} \end{bmatrix} = \begin{bmatrix} \mathbf{0} & \overline{\mathbf{G}}_0^{(P-1)} & \cdots & \overline{\mathbf{G}}_{U-2}^{(P-1)} \\ \mathbf{G}_{U-1}^{(P)} & \mathbf{G}_0^{(P)} & \cdots & \mathbf{G}_{U-2}^{(P)} \end{bmatrix} \\ &= \begin{bmatrix} \mathbf{0} & \overline{\mathbf{Q}}^{(P-1)}\overline{\mathbf{R}}_0^{(P-1)} & \cdots & \overline{\mathbf{Q}}^{(P-1)}\overline{\mathbf{R}}_{U-2}^{(P-1)} \\ \mathbf{G}_{U-1}^{(P)} & \mathbf{G}_0^{(P)} & \cdots & \mathbf{G}_{U-2}^{(P)} \end{bmatrix} \\ &= \begin{bmatrix} \mathbf{0} & \overline{\mathbf{Q}}^{(P-1)} \\ \mathbf{I}_{N_r(N_c+N_g)} & \mathbf{0} \end{bmatrix} \begin{bmatrix} \mathbf{G}_{U-1}^{(P)} & \mathbf{G}_0^{(P)} & \cdots & \mathbf{G}_{U-2}^{(P)} \\ \mathbf{0} & \overline{\mathbf{R}}_0^{(P-1)} & \cdots & \overline{\mathbf{R}}_{U-2}^{(P-1)} \end{bmatrix} \\ &= \begin{bmatrix} \mathbf{0} & \overline{\mathbf{Q}}^{(P-1)} \\ \mathbf{I}_{N_r(N_c+N_g)} & \mathbf{0} \end{bmatrix} \mathbf{Q}^{(P)}\mathbf{R}^{(P)}\end{aligned} \tag{22}$$

The expanded received signal vector after the cancelation of successfully received data $\tilde{\mathbf{Y}}^{(P,n_b)}$ of Equation (21) can be transformed as

$$\begin{aligned}\hat{\mathbf{Y}}^{(P,n_b)} &= \left\{\begin{bmatrix} \mathbf{0} & \overline{\mathbf{Q}}^{(P-1)} \\ \mathbf{I}_{N_r(N_c+N_g)} & \mathbf{0} \end{bmatrix} \mathbf{Q}^{(P)}\right\}^H \tilde{\mathbf{Y}}^{(P,n_b)} \\ &= \left\{\mathbf{Q}^{(P)}\right\}^H \begin{bmatrix} \hat{\mathbf{Y}}^{(P-1,n_b)} - \overline{\mathbf{R}}_{U-1}^{(P-1)}\mathbf{s}_{U-1}^{(n_{U-1},n_b)}) \\ \mathbf{Y}^{(P,n_b)} \end{bmatrix} \\ &= \mathbf{R}^{(P)} \begin{bmatrix} \mathbf{s}_{U-1}^{(n_{U-1}+1,n_b)} \\ \mathbf{s}_0^{(n_0,n_b)} \\ \vdots \\ \mathbf{s}_{U-2}^{(n_{U-2},n_b)} \end{bmatrix}\end{aligned} \tag{23}$$

From Equation (23), the ordering can also be realized by exchanging the columns of expanded channel matrix and transmit symbol vector in case 2 for R-QRPC.

4. COMPUTER SIMULATION RESULTS

The performance of SC MU-MIMO HARQ with QRM-MLBD using R-QRPC is evaluated by computer simulation. The simulation condition is summarized in Table I. For data modulation, 16QAM is used. We assume $U = 2$, $N_r = 2$, $N_c = 64$, $N_g = 16$, and $L = 16$-path frequency-selective block Rayleigh fading channel with uniform power delay profile. Independent channel is assumed for each retransmission. The ideal channel estimation is assumed at the receiver. A rate 1/3 turbo encoder using two $(13, 15)_8$ recursive systematic convolutional component encoders is used for channel encoder. The two parity sequences from the turbo encoder are punctured to obtain rate-3/4 turbo codes. Log-MAP decoding with six iterations is used. The packet size is set to 1024 bits, which results in $N_b = 4$ blocks per packet. An error-free ACK/NACK feedback is assumed from the receiver to each user. Maximum number of retransmissions is set to be five. Slow transmit power control is considered such that the average received powers of all the users are assumed to be the same.

4.1. Case 1

The average PER performance of SC MU-MIMO HARQ achieved by the QRM-MLBD with the R-QRPC is plotted as a function of the average received energy per symbol-to-noise power spectrum density ratio (E_s/N_0). The comparison of detection ordering schemes is shown in Figure 3. The number of surviving paths in M-algorithm is set to $M = 16$. The same packet is assumed to be transmitted $P = 2$ times. As in Figure 3 that when $P = 1$, better

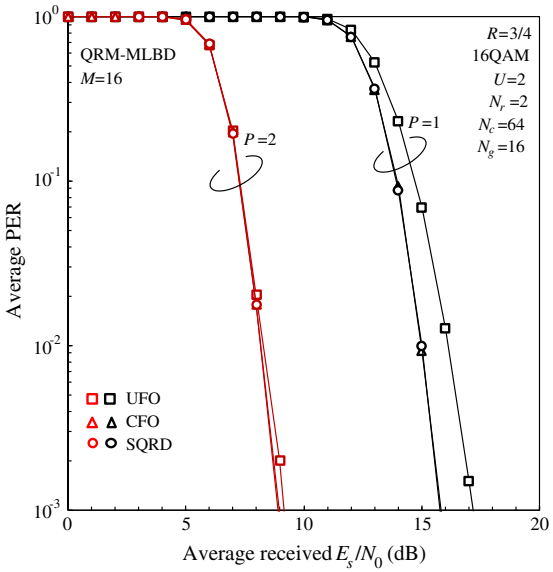

Figure 3. Comparison of detection ordering schemes (case 1). PER, packet error rate; QRM-MLBD, QR decomposition and M-algorithm-based near maximum likelihood block detection; QAM, quadrature amplitude modulation; SQRD, sorted QR decomposition.

PER performance can be achieved by using the CFO and SQRD. This is because the probability of removing the correct path at early stages is reduced. On the other hand, when $P = 2$, no performance difference among ordering schemes exists. This is because large packet combining gain can be achieved. As a result, the probability of discarding the correct path at early stages can be reduced. In the followings, the CFO is used for case 1 because of its low computational complexity.

Figure 4 shows the comparison between the R-QRPC and the bit-level LLR combining for case 1. The number

Table I. Computer simulation condition

Transmitter	Data modulation	16QAM
	No. of users	$U = 2$
	Data symbol block length	$N_c = 64$
	TS lengths	$N_g = 16$
Turbo coding	Packet size	1024
	Encoder	(13, 15) RSC encoders
	Decoder	Log-MAP decoding with 6 iterations
	Coding rate	$R = 3/4$
HARQ	Type	Type I
Channel	Fading type	Frequency-selective block Rayleigh
	Power delay profile	$L = 16$-path uniform power delay profile
Receiver	No. of receive antennas	$N_r = 2$
	Channel estimation	Ideal

HARQ, hybrid automatic repeat request; QAM, quadrature amplitude modulation; RSC, recursive systematic convolutional.

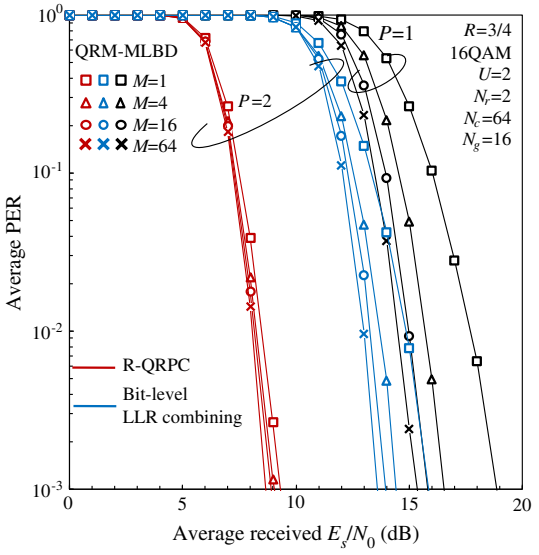

Figure 4. Comparison between recursive QR packet combining and the bit-level LLR combining (case 1). PER, packet error rate; QRM-MLBD, QR decomposition and M-algorithm-based near maximum likelihood block detection; QAM, quadrature amplitude modulation; LLR, log likelihood ratio.

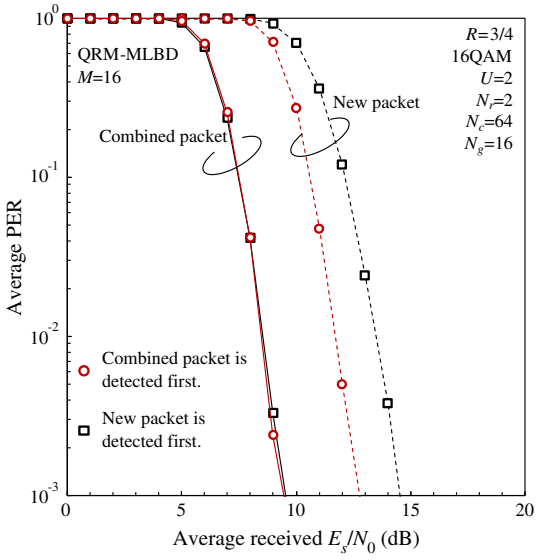

Figure 5. Comparison of detection ordering schemes (Case2). PER, packet error rate; QRM-MLBD, QR decomposition and M-algorithm-based near maximum likelihood block detection; QAM, quadrature amplitude modulation.

of surviving paths in M-algorithm is parameterized and set to $M = 1, 4, 16$, and 64. The same packet is assumed to be transmitted $P = 2$ times. As in Figure 4, the R-QRPC can achieve significantly better PER performance compared to the bit-level LLR combing. This is because the optimal packet combing gain can be obtained. The R-QRPC can reduce the required E_s/N_0 to achieve PER$= 10^{-2}$ by about 5.5 dB for $M = 4$ compared to the bit-level LLR combining. Figure 4 also shows that the achievable PER of SC MU-MIMO with the QRM-MLBD using the R-QRPC is almost the same regardless of the value of M due to large packet combining gain. As a result, the probability of removing the correct path at early stages can be reduced. This implies that in the retransmission, the receiver can reduce the value of M.

4.2. Case 2

Figure 5 shows the average PER performance achieved by the QRM-MLBD using the R-QRPC with $M = 16$ for case 2 (one user retransmits the same packet and another user transmits a new packet). Two detection ordering schemes are considered: 'the combined packet is detected first' and the other is 'the new packet is detected first'. Figure 5 shows that the PER performance of new packet is improved if it is detected later. This is because the probability of correct detection is increased because the new packet is located at the later stage of the M-algorithm. On the other hand, no performance difference among ordering schemes exists for the combined packet. This is because large packet combining gain can be achieved.

Figure 6 shows the comparison between the R-QRPC and the bit-level LLR combining for case 2. The same packet is assumed to have been transmitted $P = 2$ times. It can be seen from Figure 6 that the R-QRPC provides significantly better PER performance than the bit-level LLR combing for both new packet and combined packet. The R-QRPC can reduce the required E_s/N to achieve PER $= 10^{-2}$ by about 4.5 and 3.5 dB for combined packet and new packet, respectively.

4.3. Throughput performance

Figure 7 plots the throughput performance achieved by the QRM-MLBD using the R-QRPC for $M = 1, 4, 16$, and 64. We use the CFO for case 1 and the detection ordering in which the packet with the larger of retransmissions is detected first for case 2. The throughput performance using QRM-MLBD with the bit-level LLR packet combining is plotted for comparison. The throughput η (bps/Hz) is defined as

$$\eta = \log_2 X \times R \times \frac{1}{\overline{Q}} \times \frac{1}{1 + N_g/N_c} \tag{24}$$

where X is the modulation level ($X = 16$ for 16QAM) and $\overline{Q} - 1$ is the average number of packet retransmissions. It can be seen from Figure 7 that the R-QRPC provides significantly higher throughput performance than the bit-level LLR combing in a low E_s/N region where packet combining gain plays important role as retransmission occurs with high probability. The R-QRPC can achieve about 1.6 times higher throughput than the bit-level LLR combining when

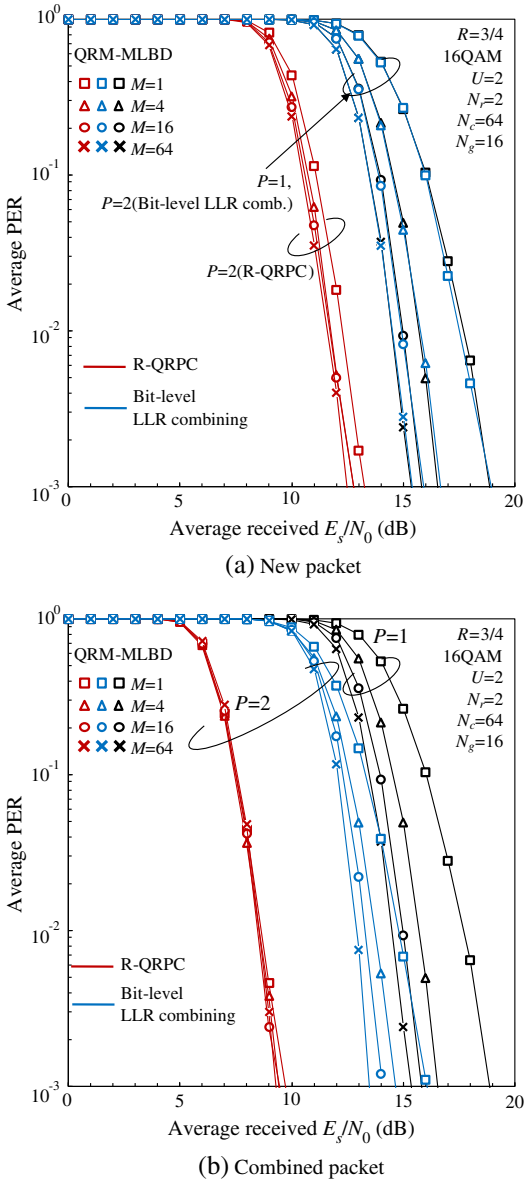

Figure 6. Comparison between recursive QR packet combining and the bit-level LLR combining (case 2). PER, packet error rate; QRM-MLBD, QR decomposition and M-algorithm-based near maximum likelihood block detection; QAM, quadrature amplitude modulation; LLR, log likelihood ratio.

$M = 4$. Figure 7 also shows that in a low E_s/N region the achievable throughput of the R-QRPC is almost the same regardless of the value of M.

5. CONCLUSION

In this paper, we presented the QRM-MLBD with the R-QRPC for MU-MIMO HARQ. Different from SU-MIMO HARQ, the received signal may consist of both new packet and retransmitted packet as the retransmission protocol

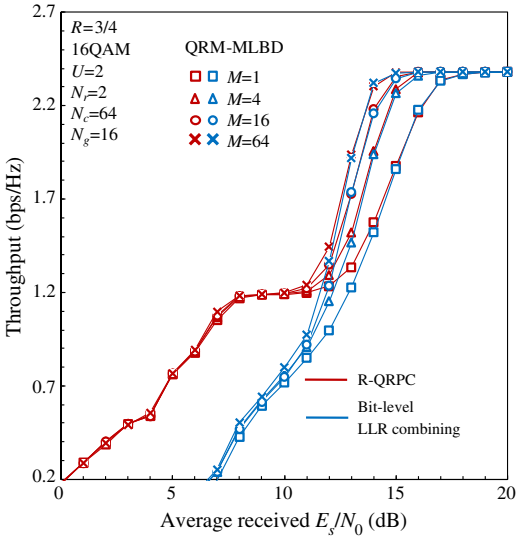

Figure 7. Throughput performance. QRM-MLBD, QR decomposition and M-algorithm-based near maximum likelihood block detection; QAM, quadrature amplitude modulation; LLR, log likelihood ratio.

independently works at each user. To improve the detection performance by taking into account this fact, the R-QRPC was derived. A detection ordering scheme was also proposed to improve quality for the case when received signal consists of both new packet and retransmitted packet. We showed by computer simulation that our proposed R-QRPC provides significantly better PER and throughput performance than the bit-level LLR combing and that the proposed new ordering scheme improves the PER performance.

REFERENCES

1. Foschini GJ, Gans MJ. On limits of wireless communications in a fading environment when using multiple antennas. *Wireless Personal Communications* 1998; **6**(3): 311–335.
2. Ekstrom H, Furuskar A, Karlsson J, Meyer M, Parkvall S, Torsner J, Wahlqvist M. Technical solutions for the 3G long-term evolution. *IEEE Communications Magazine* 2006; **44**(3): 38–45.
3. Benjamin N, Chan-Tong L, Falconer D. Turbo frequency domain equalization for single-carrier broadband wireless systems. *IEEE Transactions on Wireless Communications* 2007; **6**(2): 759–767.
4. Higuchi K, Kawai H, Maeda N, Taoka H, Sawahashi M. Experiments on real-time 1-Gb/s packet transmission using MLD-based signal detection in MIMO-OFDM broadband radio access. *IEEE Journal on Selected Areas in Communications* 2006; **24**(6): 1141–1153.

5. 3GPP, TS 36.211 (V10.4.0), 3rd Generation Partnership Project (3GPP); Evolved Universal Terrestrial Radio Access (E-UTRA); Physical Channels and Modulation (Release 10), December 2011.
6. Proakis JG, Salehi M. *Digital Communications*, (5th edn). McGraw-Hill: New York, 2008.
7. Nagatomi K, Higuchi K, Kawai H. Complexity reduced MLD based on QR decomposition in OFDM MIMO multiplexing with frequency domain spreading and code multiplexing, In *Proceedings of the IEEE Wireless Communications and Networking Conference (WCNC 2009)*, Budapest, Hungary, April 2009; 1–6.
8. Yamamoto T, Takeda K, Adachi F. Training sequence-aided QRM-MLD block signal detection for single-carrier MIMO spatial multiplexing, In *Proceedings of the 2011 IEEE International Conference of Communications*, Kyoto, Japan, June 2011; 1–5.
9. Spencer QH, Peel CB, Swindlehurst AL, Haardt M. An introduction to the multi-user MIMO downlink. *IEEE Communications Magazine* 2004; **42**(10): 60–67.
10. Sfar S, Murch RD, Letaief KB. Layered space–time multiuser detection over wireless uplink systems. *IEEE Transactions on Wireless Communications* 2003; **2**(4): 653–668.
11. Itagaki M, Takeda K, Adachi F. Frequency-domain QRM-MLD block signal detection for single-carrier multi-user MIMO uplink, In *Proceedings of the 2010 International Conference on Network Infrastructure and Digital Content (IC-NIDC2010)*, Beijing, China, September 2010; 687–691.
12. Chase D. Code combining—a maximum-likelihood decoding approach for combining an arbitrary number of noisy packets. *IEEE Transactions on Communications* 1985; **33**(5): 385–393.
13. Lee J, Toumpakaris D, Jang EW, Lou HL. DFE-based receiver implementation for MIMO systems employing hybrid ARQ, In *Proceedings of the IEEE Global Communications Conference, Exhibition, and Industry Forum*, New Orleans, LA, USA, November-December 2008; 1–5.
14. Yamamoto T, Takeda K, Adachi F. HARQ throughput enhancement using maximum likelihood block detection with recursive QR packet combining and M-algorithm for single-carrier MIMO, In *Proceedings of the 8th International Workshop on Multi-Carrier Systems & Solutions (MC-SS 2011)*, Herrsching, Germany, May 2011; 1–5.
15. Jang EW, Lee J, Lou H, Cioffi JM. Optimal combining schemes for MIMO systems with hybrid ARQ, In *Proceedings of the IEEE International Symposium on Information Theory*, Nice, France, June 2007; 2286–2290.
16. Deneire L, Gyselinckx B, Engels M. Training sequence versus cyclic prefix—a new look on single carrier communication. *IEEE Communications Letters* 2001; **5**(7): 292–294.
17. Adachi F, Obara T, Yamamoto T. Capacity and BER performance considerations on single-carrier frequency-domain equalization, In *Proceedings of the 8th International Conference on Information, Communications, and Signal Processing (ICICS 2011)*, Singapore, December 2011; 1–5.
18. Shin W, Kim H, Son M, Park H. An improved LLR computation for QRM-MLD in coded MIMO systems, In *Proceedings of the IEEE 66th Vehicular Technology Conference (VTC2007-Fall)*, Baltimore, MD, USA, September–October 2007; 447–451.
19. Kawai H, Higuchi K, Maeda N, Sawahashi M, Ito T, Kakura Y, Ushirokawa A, Seki H. Likelihood function for QRM-MLB suitable for soft-decision turbo decoding and its performance for OFCDM MIMO multiplexing in multipath fading channel. *IEICE Transactions on Communications* 2005; **E88-B**(1): 47–57.
20. Wübben D, Rinas J, Böhnke R, Kühn V, Kammeyer K-D. Efficient algorithm for detecting layered space–time codes, In *Proceedings of the 4th International ITG Conference on Source and Channel Coding (SCC)*, Berlin, Germany, January 2002; 1–7.

AUTHORS' BIOGRAPHIES

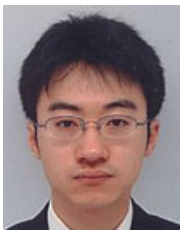

Tetsuya Yamamoto received his BS degree in Electrical, Information, and Physics Engineering in 2008, and MS and Dr. Eng. degrees in communications engineering from Tohoku University, Sendai, Japan, in 2010 and 2012, respectively. Currently, he is a Japan Society for the Promotion of Science (JSPS) postdoctoral research fellow at the Department of Communications Engineering, Graduate School of Engineering, Tohoku University. His research interests include frequency-domain equalization and signal detection techniques for mobile communication systems. He was a recipient of the 2008 IEICE RCS (Radio Communication Systems) Active Research Award and Ericsson Best Student Award 2012.

Koichi Adachi received the BE, ME, and PhD degrees in engineering from Keio University, Japan, in 2005, 2007, and 2009, respectively. From 2007 to 2010, he was a Japan Society for the Promotion of Science (JSPS) research fellow. Currently, he is with the Institute for Infocomm Research,

A*STAR, in Singapore. His research interests include cooperative communications. He was the visiting researcher at City University of Hong Kong in April 2009 and the visiting research fellow at University of Kent from June to August 2009.

Sumei Sun obtained the BSc (Honours) degree from Peking University, China, the MEng Degree from Nanyang Technological University, and PhD degree from National University of Singapore. She's been with Institute for Infocomm Research (formerly Centre for Wireless Communications) since 1995, and she is currently Head of Modulation and Coding Dept., developing physical layer-related solutions for next-generation communication systems. Her recent research interests are in energy efficient multiuser cooperative MIMO systems, joint source-channel processing for wireless multimedia communications, and wireless transceiver design.

Dr. Sun has served as the TPC Chair of 12th IEEE International Conference on Communications in 2010 (ICCS 2010), general co-chair of the Seventh and Eighth IEEE Vehicular Technology Society Asia Pacific Wireless Communications Symposium (APWCS), and track co-chair of Transmission Technologies, IEEE VTC 2012 Spring. She is an associate editor of IEEE Transactions on Vehicular Technology, and editor of IEEE Wireless Communication Letters. She is co-recipient of IEEE PIMRC'2005 Best Paper Award.

Fumiyuki Adachi received the BS and Dr. Eng. degrees in electrical engineering from Tohoku University, Sendai, Japan, in 1973 and 1984, respectively. In April 1973, he joined the Electrical Communications Laboratories of Nippon Telegraph and Telephone Corporation (now NTT) and conducted various types of research related to digital cellular mobile communications. From July 1992 to December 1999, he was with NTT Mobile Communications Network, Inc. (now NTT DoCoMo, Inc.), where he led a research group on wideband/broadband CDMA wireless access for IMT-2000 and beyond. Since January 2000, he has been with Tohoku University, Sendai, Japan, where he is a professor of communications engineering at the Graduate School of Engineering. In 2011, he was appointed as distinguished professor. His research interest is in the areas of wireless signal processing and networking including broadband wireless access, equalization, transmit/receive antenna diversity, MIMO, adaptive transmission, channel coding, etc. From October 1984 to September 1985, he was a UK SERC visiting research fellow in the Department of Electrical Engineering and Electronics at Liverpool University.

Dr. Adachi is an IEEE Fellow and a VTS distinguished lecturer for 2011 to 2013. He was a co-recipient of the IEEE Vehicular Technology Transactions Best Paper of the Year Award 1980 and again 1990 and also a recipient of Avant Garde award 2000. He is a fellow of Institute of Electronics, Information and Communication Engineers of Japan (IEICE) and was a recipient of IEICE Achievement Award 2002 and a co-recipient of the IEICE Transactions Best Paper of the Year Award 1996, 1998, and again 2009. He was a recipient of Thomson Scientific Research Front Award 2004, Ericsson Telecommunications Award 2008, Telecom System Technology Award 2009, and Prime Minister Invention Prize 2010.